

DEVELOPMENT OF A 12% CR STEEL ROTOR FORGING FOR GEOTHERMAL POWER PLANTS

M. KAMADA¹, M. SAITO¹, A. FUJITA¹, K. URA², ANDY OKAMURA³

¹Nagasaki R&D Center, Mitsubishi Heavy Industries, Ltd., Nagasaki, Japan
²Nagasaki Shipyard & Machinery Works, Mitsubishi Heavy Industries, Ltd., Nagasaki, Japan
³R&D Dept., Japan Casting & Forging Co., Kitakyushu, Japan

SUMMARY — In order to increase the stress corrosion cracking (SCC) resistance of geothermal turbine rotor materials, a new 12%Cr steel has been developed. A fundamental study of the effect of alloying elements on SCC resistance was carried out, and an alloy composition of **Fe-0.04%²C-12%Cr-5%Ni-0.05%N** was selected. Verification tests conducted on a full size turbine rotor forging showed excellent results.

1. INTRODUCTION

Low alloy steels featuring **1%Cr-1%Mo-0.25%V** (CrMoV steel) have been used for turbine rotors in geothermal power plants. CrMoV steel is one of the most commonly used materials for large-scale machine parts such as turbine rotors due to high productivity, high hardenability of the metal matrix, and a good combination of strength and ductility.

In some geothermal power plants, however, stress corrosion cracking (SCC) of turbine rotors has occurred because of the severe corrosive characteristics of geothermal steam. Changing the steel type from low alloy to 12%Cr is an effective means of increasing the SCC resistance of turbine rotor materials (Priante and Gallegari, 1981; Schonfeld et al., 1986). Mitsubishi Heavy Industries, Ltd. had already developed 12%Cr rotor steels for fossil-fueled ultra super critical (USC) steam turbines (Hizume et al., 1986, 1987; Kamada et al., 1995) and based on this experience, we have developed a new 12%Cr steel for use in geothermal turbine rotors.

A fundamental study of the effect of alloying elements on SCC resistance was initially carried out. A substantial number of ingots of 12%Cr steel alloys was prepared by means of 50kg vacuum induction melting and then they were subjected to SCC testing and heat treatment testing. As a result of this fundamental study, the alloy composition of **Fe-0.04%²C-12%Cr-5%Ni-0.05%N** was selected as being the best composition for geothermal turbine rotor material having high SCC resistance.

A full size turbine rotor forging (23.6 tons in weight) with the selected alloy composition was produced, and verification tests were carried out on productivity and material properties. No major segregation of alloying elements was observed. Mechanical properties, which were checked at

several regions of the rotor forging, satisfied the standard values. These results indicate that the new 12%Cr steel rotor forging is suitable for geothermal power plants.

2. FUNDAMENTAL STUDY

2.1 Experimental Procedure

The chemical compositions of steels used in this fundamental study are listed in Table 1. All of the ingots were prepared by means of 50kg vacuum induction melting and forged into bars 65 x 65 x 650mm in size. The steels of group A were subjected to simple corrosion testing and SCC testing in order to clarify the effect of alloying elements on corrosion and SCC resistance. Samples of CrMoV and TMK1, consisting of low alloy geothermal turbine rotor steel and 12%Cr USC turbine rotor steel, respectively, were compared. The steels of group B are based on the composition corresponding to A-6, with varied amounts of Ni. These steels were subjected to heat treatment testing in order to control the microstructures.

Corrosion test specimens (ø50mm x 3mm²) and SCC test specimens (as shown in Figure 1) were placed in the geothermal steam of a power plant for a period of two years, and the corrosion rate was calculated from the difference in weight before and after testing. SCC resistance was evaluated by observing the cross-sections of notches in the specimens to determine the presence or absence of cracks.

In heat treatment testing, group B steels were heated up to 1000° C and quenched to room temperature by air cooling. The quenched steels were tempered at 550-630° C, after which the microstructures were observed. The amount of austenite phase was determined by means of an X-ray technique, comparing the diffraction peaks of ferritic iron and austenitic iron.

Table 1 Chemical compositions of steels used in fundamental study (mass %)

	C	Si	Mn	P	S	Cu	Ni	Cr	Mo	V	N
A-1	0.035	0.18	0.50	0.014	0.002	0.01	5.38	11.84	0.99	0.025	0.037
A-2	0.047	0.18	0.50	10.012	0.001	0.01	7.02	11.98	1.00	10.024	10.056
A-3	10.043	0.18	0.51	10.013	10.002	0.01	5.47	11.91	1.97	10.026	0.054
A-4	0.039	0.16	0.50	0.014	0.002	0.01	3.42	9.95	0.99	0.023	0.005
A-5					0.002	0.01	5.49	11.97	1.00	0.024	0.021
A-6	0.030	0.17	0.50	0.012	0.002	0.01	5.35	11.95	0.99	0.026	0.461
A-7	0.031	0.16	0.50	0.013	0.002	0.49	5.44	11.92	0.99	0.025	0.042
B-1	0.096	0.18	0.50	0.013	0.002	0.01	3.45	12.02	1.00	0.026	0.043
B-2	0.100	0.18	0.49	0.013	0.002	0.01	5.00	11.88	0.98	0.026	0.040
CrMoV	10.250	0.24	0.82	0.006	10.002	—	0.33	1.21	1.11	10.250	—
TMKI	10.140	0.07	0.48	10.008	0.002	0.02	0.60	10.42	1.49	0.170	—
A6-1	0.04	0.06	0.49	0.012	0.003	—	4.54	11.97	1.00	—	0.043
A6-2	0.04	0.06	0.49	0.012	0.003	—	5.18	11.99	0.99	—	0.043
A6-3	0.04	0.06	0.49	0.014	0.004	—	6.07	11.91	0.99	—	0.044
A6-4	0.04	0.06	0.49	0.013	0.004	—	6.50	11.94	0.98	—	0.044

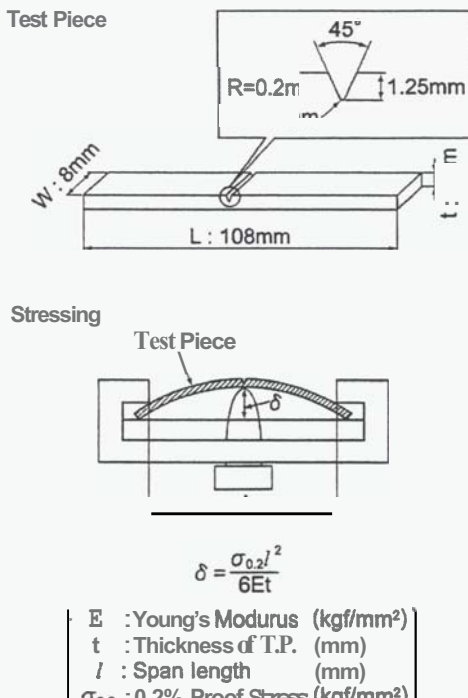


Figure 1 SCC test specimen

22 Results & Discussion

Table 2 shows the results of corrosion testing and SCC testing, and Figure 2 shows the cross sections of typical SCC test specimens. When comparing the corrosion rate of low alloy steel (CrMoV) and 12Cr steels, that of the former was found to be much higher. In the case of 12Cr steels, however, even when alloy elements such as Ni and Mo were varied, there was no great difference in the corrosion rate. On the other hand, as alloy elements were found to have substantial impact on SCC resistance, suitability differed widely among the different varieties. Differences were particularly striking

Table 2 Results of corrosion testing and SCC testing (2 years testing)

	Corrosion (mm/years)	Rate	Sensibility to SCC
A-1	0.007	◎	A
A-2	0.008	◎	O
A-3	0.007	◎	O
A-4	0.004	◎	x
A-5	0.007	◎	A
A-6	0.008	◎	O
A-7	0.007	◎	O
B-1	0.006	◎	A
B-2	0.007	◎	x
CrMoV	0.118	◎	x
TMKI	0.003	◎	A

for C and N, and SCC resistance was improved by reducing C and increasing N. Thus, based on consideration of anti-corrosion and SCC resistance, A-6 and A-7 were deemed to be appropriate compositions.

The control of material microstructure is one of the most important points in producing sound turbine rotor forgings. It was therefore necessary to confirm that the requisite microstructures could be obtained for the selected alloys at each stage of heat treatment.

Figure 3 shows a typical heat treatment pattern and desirable microstructures at each stage. At the solution treatment stage 1, the microstructure must consist of full austenite that does not include a δ -ferrite phase. This is because inclusion of the δ -ferrite phase causes a loss of toughness in the material. Detailed results are not presented here, but group B steels include substantial

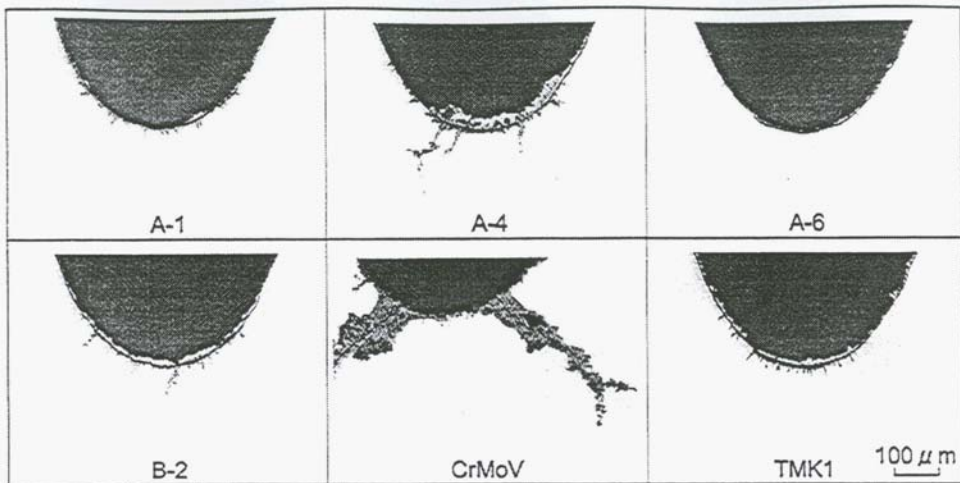


Figure 2 Cross section of typical SCC test specimens after two years testing in the geothermal steam of power plant

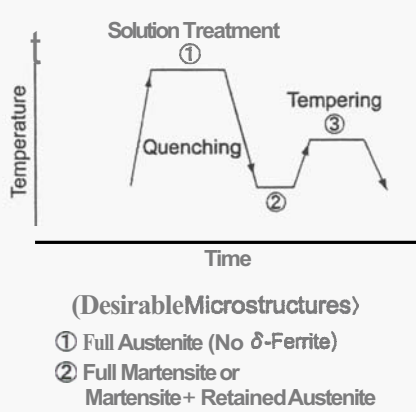


Figure 3 Typical heat treatment pattern and desirable microstructures at each stage

amounts of the austenite stabilizing element Ni, and it was confirmed that the 6-ferrite phase did not precipitate in the A6-1 alloy, which contains the least amount of Ni.

At post-quenching stage 2, the microstructure becomes either full martensite or martensite containing a small amount of retained austenite. Tempering is then performed in stage 3 in order to achieve an appropriate combination of strength and ductility. In this stage, a certain amount of martensite undergoes reverse transformation back into austenite, such that an increase occurs in the amount of austenite. If the stability of the reverse austenite is low, a phenomenon takes place in which the austenite gradually re-transforms into martensite, and there is a possibility that slight changes will take place in the dimensions of the rotor. It is necessary for reverse austenite stability to be high.

Figure 4 shows the relationship between nickel content and the amount of austenite phase in

group B steels tempered at 575°C , with the amount of austenite reaching a maximum in the vicinity of 5% nickel content. Martensite stability is higher when Ni content is under 5%, meaning that there is a smaller amount of reverse transformation to austenite. A greater amount of reverse transformation occurs at the tempering temperature when Ni content is over 5%, but, because the suppressing effect of martensite transformation induced by the material fine structure is reduced when there is excessive austenite, re-transformation of austenite to martensite occurs during cooling from the tempering temperature. This re-transformed martensite is known as fresh martensite, and has a negative influence on toughness and SCC resistance.

Figure 5 shows the effect of heat treatment on the amount of austenite phase in the A6-1 steel, with an as-quenched sample containing about 4% retained austenite. The amount of austenite increases as a result of the tempering treatment at $570\text{--}610^{\circ}\text{C}$, due to the reverse transformation of martensite to austenite. Also, the higher the tempering temperature, the greater the amount of

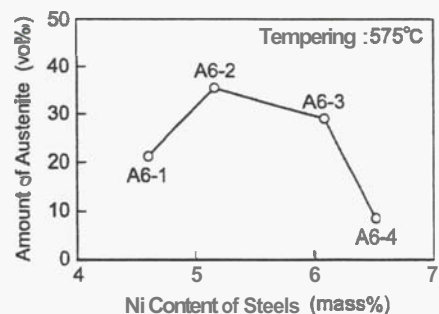


Figure 4 Relationship between nickel content and amount of austenite phase in the steels of group B tempered at 575°C .

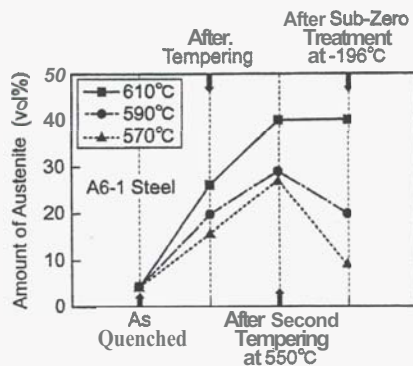


Figure 5 Effect of heat treatment on the amount of austenite phase in A6-1 steel.

austenite. Test materials subjected to double tempering treatment, involving reheating to 550°C after the first tempering treatment, were found to exhibit newly increased amounts of austenite. This indicates that reverse transformation was not completed during the first tempering treatment, pointing to the effectiveness of double tempering treatment in facilitating completion of reverse transformation. In order to investigate austenite stability following double tempering treatment, specimens were further subjected to sub-zero treatment by placing them in liquid nitrogen (-196°C). For specimens treated at tempering temperatures of 570°C and 590°C, the amount of austenite decreased. Austenite that had been stable at room temperature following double tempering treatment was observed to transform to martensite at a low temperature, suggesting a low level of austenite stability. In contrast, there was no change in the amount of austenite for specimens treated at a tempering temperature of 610°C, showing austenite stability to be extremely high.

As the result of the fundamental study, the alloy composition of Fe-0.04% C-12% Cr-5% Ni-0.05% N was selected as the best composition for the geothermal turbine rotor material with high SCC resistance.

3. PRODUCTION AND VERIFICATION STUDIES ON A FULL SIZE ROTOR

3.1 Production of the Full Size Rotor Forging

A full size rotor was produced on the basis of the knowledge obtained from the fundamental study; a production flow chart is shown in Figure 6. Ladle refining of re-ladle process was carried out after electric furnace melting to reduce impurities. The melt was cast into a 97.5 ton ingot under vacuum conditions and forged into the shape of the turbine rotor. The rotor forging was solution treated at 960°C and then quenched by blast air cooling, as shown in Figure 7. Double tempering was performed at 550°C (first tempering) and 575°C (second tempering), followed by furnace cooling. The rotor forging was then machined into its final shape, as shown in Figure 8.

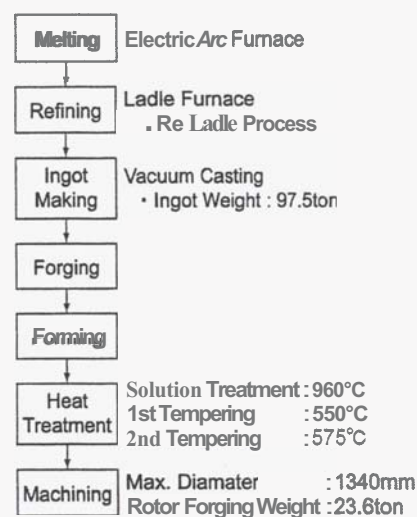


Figure 6 Production flow chart of the full size rotor

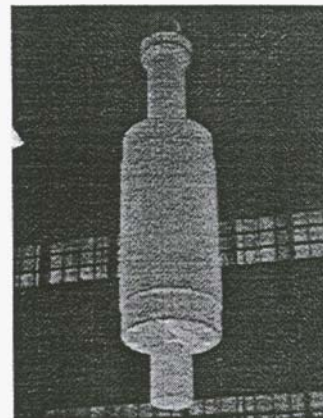


Figure 7 Full size rotor forging just before blast air cooling

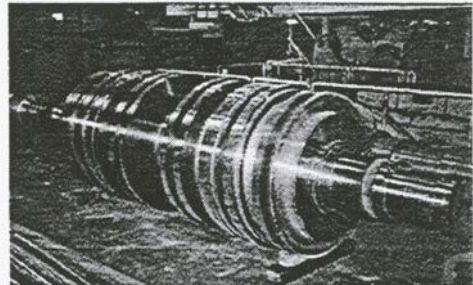


Figure 8 Full size rotor forging after machining.

32 Verification Studies on the Full Size Rotor Forging

Figure 9 shows the sampling regions of the verification test materials. Table 3 shows the chemical composition of the full size rotor forging, as ascertained at various regions. Comparison of chemical composition at each region demonstrates that segregation of alloying elements is very slight. The content of impurity elements (phosphorous, sulfur, etc.) was suppressed to the lowest level possible in industrial production.

Figure 10 shows optical micrographs of the rotor forging at various locations. The microstructure observed in Figure 10 was tempered martensite containing a considerable amount of austenite. No major differences in microstructure were found among the various locations, nor was the

harmful ferrite phase observed, thus indicating a sound microstructure. It should be noted that, because the austenite was in the form of an extremely thin film between the martensite laths, it cannot be discerned in the photograph presented here.

Figure 11 shows the macrostructure of the center core bar. Network segregation and δ -ferrite, which sometimes appear in the center of large scale 12%Cr steel ingots, were not observed in any region.

Table 4 shows the results of tensile and impact testing performed with the materials sampled from several regions of the rotor forging. Both of these properties satisfy the standard values. Toughness in particular is excellent and that the FAT" (fracture appearance transition temperature)

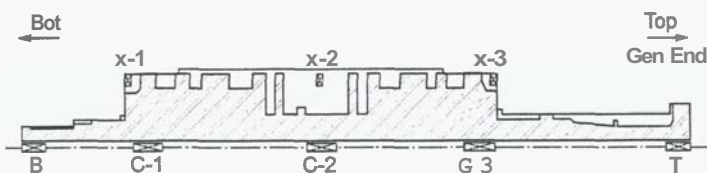


Figure 9 Sampling regions of verification test materials

Table 3 Chemical compositions of full size rotor forging at various regions (mass %)

	C	Si	Mn	P	S	Cu	Ni	Cr	Mo	V	N
X-1	0.04	0.25	0.55	0.009	0.001	0.05	5.10	11.78	1.15	0.03	0.059
X-2	0.04	0.27	0.56	0.011	0.001	0.05	5.15	11.83	1.17	0.03	10.060
X-3	0.04	0.26	0.55	0.010	0.001	0.05	5.08	11.79	1.15	0.03	0.059
B	0.04	0.26	0.55	0.010	0.001	0.05	5.07	11.73	1.15	0.03	0.060
C-1	0.04	0.26	0.56	0.010	0.001	0.05	5.07	11.78	1.16	0.03	0.059
C-2	0.04	0.26	0.55	0.010	0.001	0.05	5.07	11.74	1.13	0.03	0.060
C-3	0.05	0.27	0.57	0.011	0.001	0.05	5.12	11.79	1.16	0.03	0.060
T	0.05	0.27	0.57	0.011	0.002	0.05	5.13	11.88	1.18	0.03	0.059

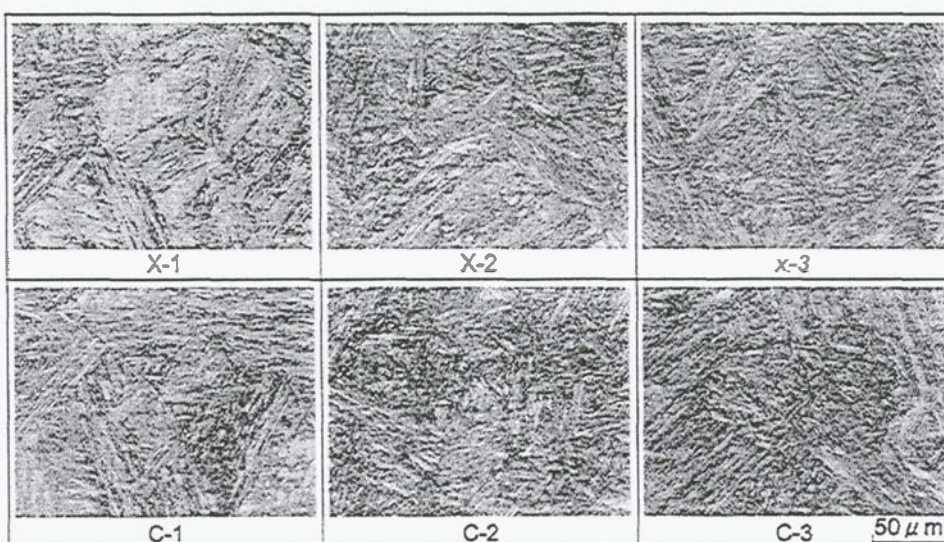


Figure 10 Optical micrographs of rotor forging at various regions

is as low as -160°C , which is due to the fact that tough austenite exists in the form of an extremely thin film between the martensite laths. There were no major differences in tensile and impact properties from region to region.

As shown above, the full size rotor forging produced in this study features excellent microstructure and mechanical properties, sufficient for use in a geothermal power plant.

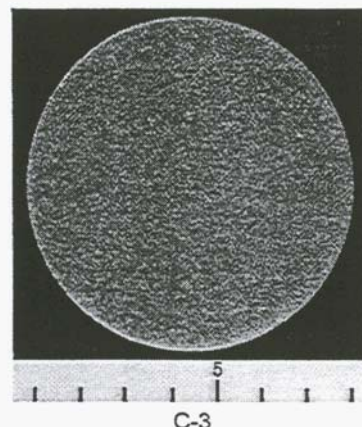


Figure 11 Macro-structure of the center core bar

Table 4 Mechanical properties of the full size rotor forging at various regions

	Tensile Testing				Impact Testing	
	0.2% Proof Stress (MPa)	Tensile Strength (MPa)	Elongation (%)	Deduction in Area (%)	Absorbed Impact Energy at 25°C (J)	50% FATT ($^{\circ}\text{C}$)
Standard	5635	≥ 740	≥ 16	≥ 45	≥ 30	S40
X-1	703	905	20.6	52.7	140, 141	-162
x-2	736	894	20.6	54.8	122, 129	-164
x-3	705	909	21.0	53.8	143, 136	-160
GI	742	892	20.6	52.7	122, 126	-167
c-2	760	894	20.6	52.7	124, 122	-182
C-3	760	905	20.0	51.6	134, 127	-172

4. CONCLUSIONS

In order to increase the stress corrosion cracking (SCC) resistance of geothermal turbine rotor materials, a new 12%Cr steel was developed. The results are summarized as follows:

- 1) The influence of C (carbon) and N (nitrogen) on the SCC resistance of 12%Cr steel is considerable, and SCC resistance was improved by simultaneously decreasing the C content and increasing the N content.
- 2) Consideration was given to microstructure changes in the heat treatment process. The combination of 5% Ni additive content with double tempering treatment was found to be effective in controlling a martensite structure that includes highly stable austenite.
- 3) Based on the foregoing fundamental study, a full size turbine rotor forging with an alloy composition of Fe-0.04% C-12% Cr-5% Ni-0.05% N was produced. The results of verification studies demonstrate that the full size rotor forging manufactured in this study has excellent microstructure and mechanical properties, sufficient for use in a geothermal power plant.

5. REFERENCES

Hizume, A., Takada, Y., Yokota, H., Takano, Y., Suzuki, A., Kinoshita, S., Koono, M. & Tsuchiyama, T. (1986) ASME Winter Annual Meeting, Anaheim, CA Dec. 7-12

Hizume, A., Takada, Y., Yokota, H., Takano, Y., Suzuki, A., Kinoshita, S., Koono, M. & Tsuchiyama, T. (1987) Advances in Material Technology for Fossil Power Plants. Chicago p 143-151.

Kamada, M., Fujita, A., Takano, Y., Fujikawa, T., Yokota, H., Tsuchiyama, T. & Miyakawa, M. (1995) 3rd International Charles Parsons Turbine Conference, Newcastle, UK, Apr. 25-27 p 181-189.

Priante, M. and Gallegari, I. (1981) International Forging Conference, Dusseldorf

Schonfeld, K. and Potthast, V. (1986): Steel Forging ASTM STP903, p143-154